MRS Advances © 2019 Materials Research Society
DOI: 10.1557/adv.2019.386

Carbon Nanotube Fabric-Based Composites for Development of Multifunctional Structures

Michael B. Jakubinek[1]*, Yadienka Martinez-Rubi[1], Behnam Ashrafi[2], Nicholas Gumienny-Matsuo[1], Daesun Park[2], Hao Li[1], Stéphane Dénommée[1] and Benoit Simard[1]*

[1]*Division of Emerging Technologies, National Research Council Canada, Ottawa, Ontario, Canada*

[2]*Aerospace Research Centre, National Research Council Canada, Montreal, Quebec, Canada*

*Corresponding author emails: Michael.Jakubinek@nrc-cnrc.gc.ca, Benoit.Simard@nrc-cnrc.gc.ca

ABSTRACT

Carbon nanotubes (CNTs) possess impressive properties along with low density. Integration of CNTs in the form of fabrics or other preformed assemblies simplifies their handling and allows for the higher CNT content needed to better leverage their properties in multifunctional structures. Here we describe production of non-woven CNT-polyurethane fabrics made from industrial-grade CNTs via a one-step filtration method. Individual sheets were scaled to 30 cm x 30 cm size and subsequently used to fabricate thicker composites, including via lamination with itself to produce simple panels and with other materials to further tailor the nanocomposite properties and address several example applications including electrical heating, fire resistance, electromagnetic shielding, and a skin for stretchable morphing structures.

INTRODUCTION

Carbon nanotubes (CNTs), which are renowned for their exceptional properties, low density and nanoscale structure, are now manufactured commercially in large quantities and are appearing in an increasing range of CNT-enhanced or CNT-enabled products [1]. The most common approaches to produce CNT composites involve dispersion of relatively low quantities of CNTs, up to a few percent by weight (wt.%), in a matrix. Although CNTs have seen relatively less impact on textile products thus far, new advances in production of nonwoven CNT fabrics, which are often called buckypaper in

the nanotube literature, are poised to make an impact in nano-engineered textiles [2]. In contrast to dispersion methods, forming a macroscale assemblies of CNTs (sheets, films, fibers, *etc*.) allows for higher CNT-content, which is advantageous to better leverage the mechanical and multifunctional properties of the CNTs. It also facilitates orientation of nanotubes (unidirectionally or randomly in-plane), simplifies handling in comparison to nanomaterial powders, and can be compatible with conventional composites manufacturing processes (e.g., layup). CNT buckypaper sheets have been explored for applications including electromagnetic shielding, thermal conduction, fire retardancy and reinforcement for polymer composites [e.g., 3-9].

Recently, we reported a novel approach to produce sheets consisting of CNTs and thermoplastic polyurethane (TPU) [10]. This approach, which results in production of porous nonwoven fabrics (buckpapers) consisting of TPU-coated nanotubes, is described and scaled to produce 30 cm x 30 cm nanotube-based fabrics. Subsequently, we describe the production and properties of thicker composite panels with high CNT content (20 wt.% to 50 wt.%) via lamination of individual fabric layers. The nanocomposite is also laminated with other materials and several example applications are illustrated. The work shows a pathway to production of composite structures with high CNT content from this CNT-TPU fabric that can be applied to a variety of multifunctional composite structures.

EXPERIMENTAL

Materials & Manufacturing

Materials

CNTs used in this work were NC7000^{TM} industrial grade multi-walled carbon nanotubes (MWCNTs) purchased from Nanocyl. The thermoplastic TPU, UAF 472, was obtained as a film from Adhesive Films Inc.

Nonwoven nanocomposite fabric

Fabric sheets consisting of CNTs and TPU were produced as described in our previous publication [10]. Briefly, as illustrated in Figure 1, the CNTs were dispersed in methanol by sonication and, separately, TPU was dissolved in acetone. The dispersed CNTs were subsequently combined with the TPU solution, followed by additional sonication, and a nonwoven sheet of CNT-TPU was then recovered by vacuum filtration. The composition can be controlled by adjusting the ratio of CNTs to TPU. An important feature of this process is the combination of a nonsolvent and solvent for the TPU where, in the presence of the CNTs, the dissolved TPU forced out of solution associates with the surface of the CNTs and, over a broad range of compositions, the resulting nanocomposite sheet is a porous, non-woven fabric of TPU-coated CNTs (see Figure 2) [10].

In this case, this process was scaled to a 30 cm x 30 cm filtration setup. A stock solution of MWCNTs in methanol (20 g/ 20 L) was prepared using a flow-through tip sonicator and mechanical shaking to disperse CNTs and homogenize the stock solution. For individual sheets, 2.5 L of the stock solution (2.5 g MWCNTs) was bath sonicated for 30 minutes using a peristaltic pump to provide constant mixing. This was then added to solution of TPU in 2.5 L of acetone, where the amount TPU in solution was varied to vary the composition of the fabric. The CNT dispersion was added to the TPU solution followed by additional bath sonication/mixing, high shear homogenization and tip

sonication steps prior to vacuum filtration to recover a 30 cm x 30 cm fabric sheet. These sheets were dried for 48 hours at room temperature under compression in a hot press to prevent contraction and wrinkling during drying, followed by additional drying for 2 hours at 100 °C.

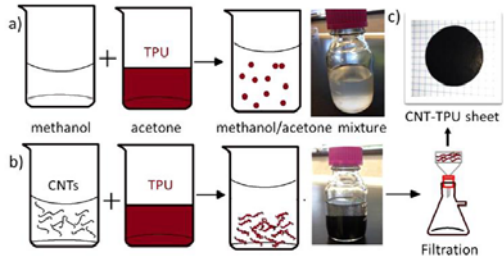

Figure 1. Illustration of the method for preparing CNT-TPU sheets. (a) TPU phase separation upon addition of the non-solvent (methanol). (b) TPU immobilization on the CNT surface. (c) Photo of a CNT-TPU sheet after filtration. Reproduced, with permission, from the authors' previous work [10].

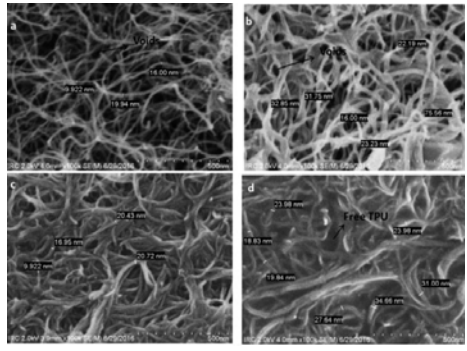

Figure 2. SEM images of the surfaces of (a) CNT buckypaper (100% CNTs) and (b) CNPU-55, (c) CNPU-65 and (d) CNPU-80 composite sheets. Reproduced, with permission, from the authors' previous work [10].

Layering and lamination

In order to produce thicker samples with high CNT content, the thin CNT-TPU fabrics were laminated by hot pressing (Carver press, max load 24,000 lbs). With the presence of the thermoplastic TPU component, it was not necessary to add additional polymer mass to produced laminated composites. In this work the large CNT-TPU fabrics were cut to smaller rectangles, which were stacked and laminated. The typical lamination steps consisted of: transfer to the hot press at 120 °C, 10 minute hold, 5 minutes under a load of 1700 psi, cooling to below 50 °C before removing the load. A range of other pressures from < 200 psi to > 2000 psi were also used in limited tests.

Characterization

Samples were assessed in terms of their mass and dimensions, morphology by SEM, and tensile properties. Tensile testing was performed on rectangular coupons (~ 30 mm x 1.5 mm x 0.1 mm) with an MTS Criterion C41 load frame with a 1 kN load cell and at a displacement rate of 10 mm/min.

RESULTS AND DISCUSSION

30 cm x 30 cm nanocomposite fabrics

Figure 3 shows photographs for 30 cm x 30 cm area (~ 100 µm thick) CNT-TPU nanocomposite fabrics. The uniformity of each sheet was assessed by micrometer measurements of thickness. Typical standard deviations from 49 measurements (7 x 7 grid pattern) were ~10% with some cases closer to 20%; however, micrometer measurements do not probe the full area and also compress the sample. Areal density was selected as a more reliable measurement of macroscale variation in the fabric. Figure 3 also shows maps of areal density for sheets with 20 wt% and 50 wt% CNTs that were cut to 3 cm x 4 cm squares, which reflects typical sizes (3 cm to 6 cm) used for preparation of laminated samples. The standard deviation in areal density across the sheet was around 6%.

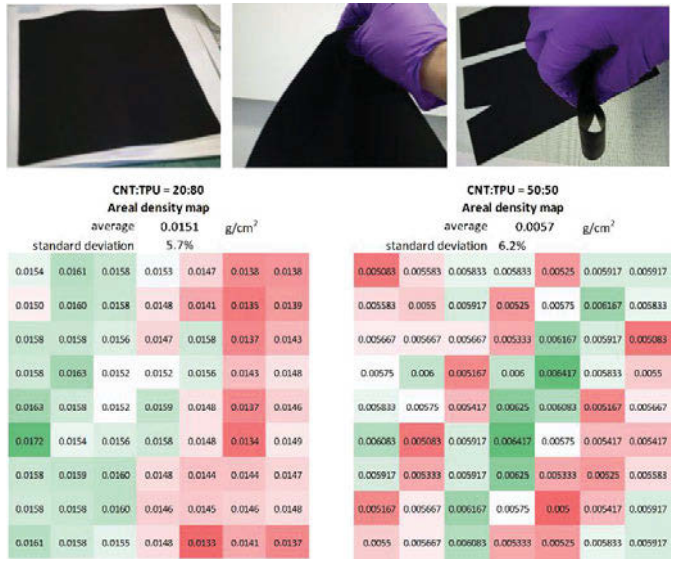

Figure 3. Larger scale, 30 cm x 30 cm, CNT-TPU fabrics. (Top) Photographs and (Bottom) areal density maps for fabrics with lower (20 wt.%) and higher (50 wt.%) CNT content.

Laminated panels

Thicker, high-CNT content composites were successfully prepared by via hot pressing (Figure 4a). For most samples the lateral dimensions were not changed by the hot pressing procedure but the thickness was reduced. Therefore the lamination procedure leads to reduced void content (higher volume% of CNTs) and increased composite density. As shown in Figure 4b, the density tended to increase with the number of layers and approach a constant value for thicker laminates. The drop in density for more than 3 layers in the case of only the 20 wt% CNT composite corresponded to lateral deformation and damage to the rectangular laminate. This suggests that when the TPU content was relatively high (80 wt.% TPU) the sample could not support the pressure and there was outward flow of material under the hot pressing conditions.

For the 35 wt% CNT laminates, which was the optimum identified in our previous report for the fabric sheets [10], the tensile properties (elastic modulus, E, ultimate tensile strength, UTS, and strain at maximum stress, ε) of the laminates were essentially equal to those of the single-layer of fabric. However, because the lamination process increased the density, the properties of the laminates were compared (see Figure 5) in terms of their specific elastic modulus ($E^* = E/\rho$) and specific ultimate tensile strength ($UTS^* = UTS/\rho$), where ρ is the laminate density. When viewed in terms of these specific properties, the tensile properties of the 35 wt.% CNT composites were reduced relative to the individual fabric layers. This change was less apparent for composites with 50 wt.% CNTs, where E* tended to be increase. The differences between these 20 wt.% to 35 wt.% to 50 wt.% composites suggest that the higher CNT content fabric can more effectively consolidate under these lamination conditions, perhaps due its lower density (higher porosity) and thinner coating of TPU on the nanotubes. However, there is significant scatter and interpretation of the 20 wt.% data is complicated by the lateral deformation of samples with more than three layers. Further exploration of composition and lamination conditions is essential to draw more definitive conclusions. Notwithstanding the preliminary nature of the results, the present study clearly shows the utility of the lamination approach to produce high CNT content TPU nanocomposites, which can be more broadly useful than the fabrics, and that the layered composite properties are competitive with the properties of the initial fabrics.

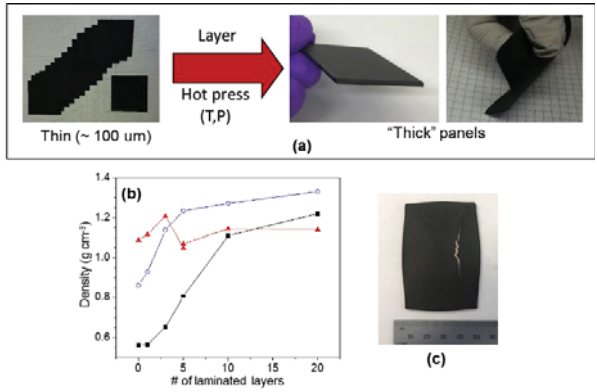

Figure 4. (a) Fabrication of a 1.2 mm thick nanocomposite panel via lamination of CNT-TPU fabric sheets. (b) Composite density as a function of CNT content (20 wt.% (▲), 35 wt.% (○) and 50 wt.% (■)) and the number of laminated sheets, where the density of the initial fabric before hot pressing is indicated on the graph as 0 sheets. (c) a 20-layer, 20 wt.% CNT sample showing in-plane deformation and damage.

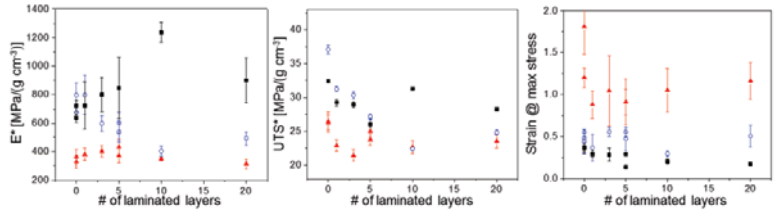

Figure 5. Specific elastic modulus, specific ultimate tensile strength, and strain at maximum stress for laminated CNT-TPU composites with 20 wt.% (▲), 35 wt.% (○) and 50 wt.% (■) CNTs. The properties of the fabric before hot pressing are indicated on the graph as 0 layers.

Example applications

The current fabric approach offers several advantages including high CNT content, convenient form factor and handling, scalability, and a thermoplastic TPU component allowing for lamination of multiple plies of CNT-TPU fabric or with other materials. Here we briefly highlight several of our current application activities to illustrate the potential of this particular CNT-based fabric for a variety of multifunctional structures.

Stretchable morphing skin

The CNT-TPU fabrics can also be laminated to the surface of other materials using the TPU as an adhesive and to layers of neat TPU. As an example of the latter, we recently described laminating CNT-TPU fabrics, in this case using a lower stiffness TPU (Tecoflex EG 80A), to either side of a TPU sheet (Duraflex PS7010) [11]. This

arrangement increased the flexural stiffness while maintaining low tensile elastic modulus and good stretchability and is being explored as a candidate for stretchable morphing structures, specifically a benchtop scale morphing wing model (Figure 6).

Internal heater for laminate manufacturing

The previous example provided an illustration of the use of this type of CNT-based fabric for surface heating. The fabric can also been adhered to other materials for surface heating. In recent years there have been several examples using CNT sheets as heaters for curing of thermoset composites [e.g., 12,13]. An advantage is that such heaters can be integral to the composite material. As a related example, the CNT-TPU fabric can be applied as in heater for manufacturing of ultra-high molecular weight polyethylene (UHMWPE) fabric laminates. Such laminates, which offer high impact resistance and are used for armor, are manufactured by hot pressing at high pressures. The requirement for heat to diffuse through this polymer material limit manufacturing speed. In the case of thick panels (e.g., 2" to 4"), it becomes impractical to heat the inner layers to sufficient pressure to achieve the desired product without overheating and degrading the outer layers. Figure 7 illustrates this challenge for a 4" thick UHMWPE fabric laminate. By inserting CNT-TPU fabric heater ever 1" through the thickness the entire laminate was heated to the required temperature quickly. The embedded heaters also show potential to fabricate thinner panels with shorter cycle times and for thermal based non-destructive inspection.

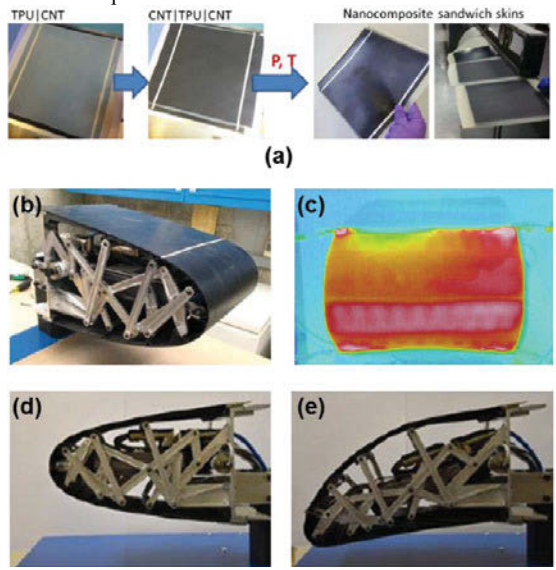

Figure 6. (a) Layering and lamination of CNT-TPU fabric layers around a sheet of neat TPU to form a "nanocomposite sandwich". A series of three nanocomposite samples are shown held flat over the edge of a benchtop and can be observed to be stiffer in bending (i.e., deflect less) than neat TPU sheets of equivalent thickness shown for comparison. We are exploring this material as (b,c) the outer surface (skin) of a stretchable, heatable morphing wing model (b: photograph and c: infrared image of NRC's morphed leading edge model). The model structure is shown in the cruise shape (d) and stretched toward a drooped shape (e). Reproduced and adapted, with permission, from the authors' previous report [11].

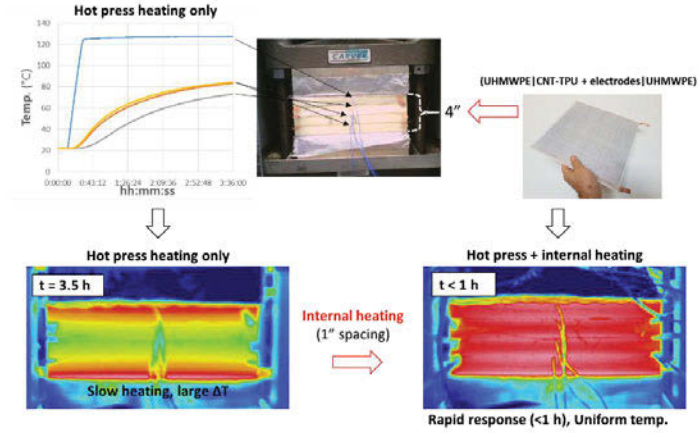

Figure 7. Use of CNT-TPU fabrics as internal heater within UHMWPE-based fabric laminates. Insertion of a heater layer at 1" intervals provides for rapid heating and uniform temperature in manufacturing of thick laminates.

Flame resistance

Due to the high content of CNTs and compatibility with UHMWPE materials, we are also evaluating the use of CNT-TPU fabric on the flame resistance of UHMWPE-based laminates used in armour and other applications. Figure 8 shows panels without and with a CNT-TPU layer after exposure to flame (UL94 flammability test). The unprotected panel ignited and must be extinguished, while the protected panel withstood the test despite the thin CNT-TPU layer being much lighter than conventional fire resistant coatings.

Electromagnetic shielding

Conductive composites based on CNTs are known to provide shielding against electromagnetic radiation [e.g., 3,14]. High CNT content as well as CNT alignment, either unidirectionally or within the plane, also improves conductivity and hence the potential for electromagnetic interference shielding. In this example a waveguide approach with a vector network analyser was employed to measure scattering parameters (S-parameters) of a network containing CNT-TPU fabrics or laminate. Nanocomposites (up to 20 layers) were clamped between aluminium plates with a window in the center and then fitted to a rectangular waveguide. S_{12}, the fraction of the signal transmitted from port 1 to port 2 of the waveguide, measured within the X-band, is shown in Figure 9. This illustrates good shielding effectiveness that increases with number of laminated layers.

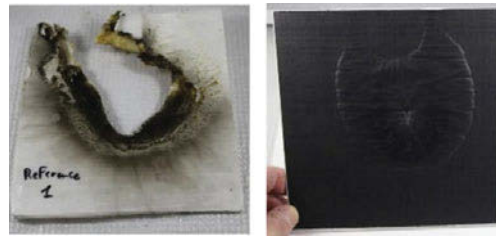

Figure 8. UHMWPE-based panels without (left) and with (right) a thin layer of CNT-TPU fabric after exposure to a flame following a UL94 flammability test.

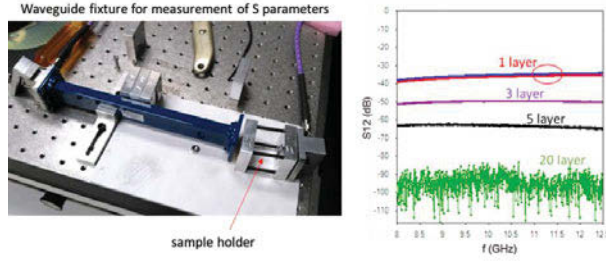

Figure 9. Assessment of shielding effectiveness via measurement of S-parameters of a network containing the CNT-TPU. The two datasets labelled "1 layer" indicate no significant difference between as-produced and hot-pressed layers.

CONCLUSIONS

Nonwoven fabrics composed of CNTs and TPU, which are a convenient form for handling and achieving high content of CNTs, were scaled to 30 cm x 30 cm size and used in lamination procedures to produce multifunctional structures. Lamination offers a route to produce thicker structures with high CNT wt% and reasonably good mechanical properties utilizing broadly available, industrial-grade CNTs. The density of the laminated composites increased with the number of layers and approached a constant value; however, the specific tensile properties (strength, or elastic modulus, divided by density) were reduced relative to the initial fabric in many instances. This may relate to degradation of the TPU or unwanted effects on the nanocomposite morphology. For example, in cases with lower CNT content and many layers, the laminates deformed irreversibly indicating pressure-induced lateral flow of material during lamination. Further exploration of lamination conditions, including temperature, pressure and time, and the TPU composition may allow for selection of conditions that will laminate the composites but prevent degradation in the tensile properties. Lamination of CNT-TPU fabrics with neat TPU layers or with other materials offers further opportunities to tailor the nanocomposite performance, and add desirable multifunctional features within or on the surface of structures, including for morphing, heating, fire resistance and shielding applications.

ACKNOWLEDGMENTS

This paper is based on an invited presentation of the same title at the 2019 International Materials Research Congress. Funding was provided by the National Research Council Canada through its *Security Materials Technology Program*. The morphing skin example was also supported by programs on *Aeronautics for the 21st Century* and *Advanced Manufacturing*. The authors are grateful to many colleagues including: C. Storey for S-parameter measurements, E. Patenaude, D. Maillard, V. Pankov and C. Li for the flame resistance test and project leadership on Fire Resistant Materials, S. Baril-Gosselin and S. Labonte for providing UHMWPE and advice, and to NRC's morphing wing project team including M. Palardy-Sim, S. Roy, M. Rahmat, F. Shadmehri, G. Renaud and others.

References:

1. M.F.L De Volder, S.H. Tawfick, R.H. Baughman, A.J. Hart. *Science* 339, 535, 2013.
2. P.D. Bradford, Creating the future of textiles: CNT fabrics. *Specialty Fabrics Review*, Sept 2013.
3. J.G., Park, J. Louis, Q. Cheng, J. Bao, J. Smithyman, R. Liang, B. Wang, C. Zhang, J.S. Brooks, L. Kramer, P. Fanchasis, D. Dorough. *Nanotechnology* 20, 415702, 2009.
4. H. Chen, M. Chen, J. Di, G. Xu, H. Li, Q. Li. *J. Phys. Chem. C*, 116, 3903, 2012.
5. Z. Wang, Z. Liang, B. Wang, C. Zhang, L. Kramer. *Compos. A* 35, 1225, 2004.
6.. B. Ashrafi, J. Guan, V. Mirjalili, P. Hubert, B. Simard, A. Johnston. *Compos. A* 41, 1184, 2010.
7. X. Fu, C. Zhang, T. Liu, R. Liang, B. Wang. *Nanotechnology* 21, 235701, 2010.
8. Q. Chen, J. Bao, J. Park, Z. Liang, C. Zhang, B. Wang. *Adv. Funct. Mater.* 19, 3219, 2009.
9. M.B. Jakubinek, B. Ashrafi, J. Guan, M.B. Johnson, M.A. White, B. Simard. *RSC Adv.* 4, 57564, 2014.
10. Y. Martinez-Rubi, B. Ashrafi, M.B. Jakubinek, S. Zou, K. Laqua, M. Barnes, B. Simard. *ACS AMI* 9, 30840, 2017.
11. M.B. Jakubinek, S. Roy, M. Palardy-Sim, B. Ashrafi, F. Shadmehri, G. Renaud, M. Barnes, Y. Martinez-Rubi, M. Rahmat, B. Simard, A. Yousfpour, F. Fortin. *AIAA SciTech Forum*, 2019-1857. doi: 10.2514/6.2019-1857 (2019)
12. B. Mas, J.P. Fernández-Blázquez, J. Duval, H. Bunyan, J.J. Vilatela. *Carbon* 63, 523, 2013.
13. J. Lee, X. Ni, F. Daso, X. Xiao, D. King, J. Sánchez Gómez. T. Blanco Varela, S.S. Kessler, B.L. Wardle. *Compos. Sci. Technol.* 166, 150, 2018.
14. J.M. Thomassin, C. Jérôme, T. Pardoen, C. Bailly, I, Huynen, C. Detremleur. *Mater. Sci. Eng R* 74, 211, 2013.